# Hydration-Induced Far-Infrared Absorption Increase in Myoglobin

**Chenfeng Zhang and Stephen M. Durbin***

*Department of Physics, Purdue University, West Lafayette, Indiana 47907*

*Received: June 7, 2006; In Final Form: September 10, 2006*

The interaction of proteins with an aqueous environment leads to a thin region of "biological water", the molecules of which have properties that differ from those of bulk water, in particular, reduced absorption of far-infrared radiation caused by protein-induced hindrance of the water rotational and vibrational degrees of freedom. New results at terahertz (THz) frequencies, however, show that absorption per protein molecule is increased by the presence of biological water. Absorption measurements were made of the heme protein myoglobin mixed with water from 3.6 to 98 wt % in the frequency range of 0.1−1.2 THz, using THz time-domain spectroscopy. Analysis shows greater THz absorption when compared to a non-interacting protein−water model. Including the suppressed absorption of biological water leads to a substantial hydration-dependent increase in absorption per protein molecule over a wide range of concentration and frequencies, meaning that water increases the protein's polarizability.

## I. Introduction

Proteins require water to function, so the role of water in protein dynamics has long been a focus of interest.[1−3] Not only does water strongly influence various physical properties of proteins,[4−6] but proteins and other biological macromolecules also influence the physical properties of water.[7−11] The region of water in the immediate vicinity of a protein surface, extending through one to two layers of water molecules, is composed of "biological water," so-called because of perturbations to the spatial arrangement, dynamics, and other physical attributes compared to bulk water.[12,13] In addition to this surface layer of biological water, proteins also include water molecules in their interiors that are even more highly constrained.[14,15]

A minimum threshold of water is required to activate the dynamics and functionality of most proteins.[1,8] For example, enzymatic activity typically requires a water content of about 20 wt %.[2,3] Some studies have indicated that the presence of water enhances the flexibility of protein molecules.[14,15] Dielectric measurements of lysozyme[14,15] and cytochrome *c*[15] powders showed an increased polarizability of the proteins due to water, which was described as a "plasticizer" that enables a larger dipole response to external electromagnetic radiation.

The interactions between biological macromolecules and water have been studied with various structural and dynamical probes such as X-ray and neutron scattering,[16−20] NMR spectroscopy,[21−24] dielectric spectroscopy,[25−28] and Fourier transform infrared (FTIR) spectroscopy.[29−31] We report here on the use of terahertz time-domain spectroscopy (THz-TDS), an extension of FTIR spectroscopy to sub-millimeter scale wavelengths. A relatively recent technique, THz-TDS exploits advances in pulsed THz sources and detectors that allow for absorption measurements up to several THz to be done with significantly improved sensitivity compared to earlier methods.[32] Water's large permanent dipole moment causes it to dominate absorption of THz radiation in most biological systems, so this technique is especially well-suited to observing protein-induced polarization changes in biological water.[33]

Although it may be possible to observe distinct absorption peaks for smaller biomolecules such as amino acids,[34,35] previous THz-TDS measurements on myoglobin (Mb), from dry powder up to 42 wt % water, established that absorption is dominated by the water content.[36] A nearly continuous absorption spectrum with increasing frequency was observed that proved to be devoid of any obvious features characteristic of Mb. This monotonically continuous absorption nature has been confirmed for other biological macromolecules such as collagen,[37] lysozyme,[38,39] cytochrome *c*,[40] bovine serum albumin (BSA),[37,41] bacteriorhodopsin (BR),[38,42] and DNA.[37,43] Quantitative measurements for Mb have now been extended to 98 wt % water, allowing a systematic look at the absorption per Mb molecule as a function of concentration. The results presented below show that total absorption exceeds that expected for non-interacting protein−water mixtures, despite the expectation that the biological water absorbs less than bulk water. After inclusion of the suppressed biological water absorption, the molar absorption of Mb in the 0.3−0.8 THz range significantly exceeds that of dry Mb for nearly all concentrations. Details of these measurements are presented in section II, and analysis in terms of hydration-induced polarizability of Mb is discussed in section III.

## II. Experiments

The sample preparation techniques and THz-TDS measurement system are extensions of those described in our prior publication covering the concentration range from 3.6 to 42 wt % water.[36] Some modifications were necessary to investigate specimens with high water content, in part due to their higher absorption at THz frequencies.

**II.1. Sample Preparation.** Horse heart Mb lyophilized powder was purchased from Sigma (lot 122K7057) and used without further purification. Mb powder samples at various hydration levels were obtained by allowing as-received lyophilized powder to equilibrate with different saturated salt solutions in desiccators over several days. The water content of the hydrated Mb powders is determined by measuring the weight loss upon heating. Using this method, we prepared Mb powders with precisely controlled hydration levels up to 42 wt %. The

* Author to whom correspondence should be addressed [e-mail durbin@physics.purdue.edu; telephone (765) 494-6426; fax (765) 494-0706].

10.1021/jp063545+ CCC: $33.50 
Published on Web 10/24/2006

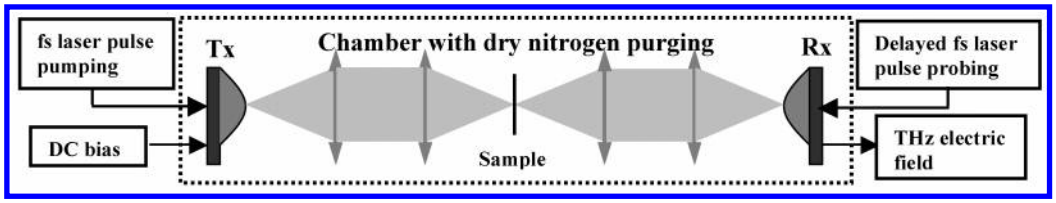


**Figure 1.** Experimental setup in a simplified version. THz optics are within the dashed box, showing the transmitter (Tx), receiver (Rx), and lenses for collecting the radiation and focusing onto the sample, all within a chamber that can be purged with dry nitrogen gas to remove water vapor absorption effects. The transmitter is pumped by fs laser pulse and biased by external DC voltage to generate the THz radiation. The receiver is probed by delayed fs laser pulse to detect the transmitted THz radiation, and the detected electric field is amplified through lock-in amplifier.

sample holder was made of two pieces of high-density polyethylene (HDPE) clamped together, with a surface recess in the center of one piece to hold the Mb powder. During the preparation of the sample, care was taken to ensure that the recess was uniformly filled with the various Mb powders. Because radiation at 1.0 THz frequency corresponds to a wavelength of ~300 $\mu$m, which is much larger than typical Mb particle sizes, elastic scattering effects from the particle are expected to be negligible.

By dissolving lyophilized Mb powder into deionized water, we produced Mb solutions with water concentrations from 70 to 98 wt %. When the water concentration of the solutions was determined, the 10 wt % water content of the lyophilized Mb powder was also taken into account. For water concentrations down to about 80 wt %, the Mb powder appeared to fully dissolve, whereas a suspension of Mb particles was visible for the samples at 75 and 70 wt % water concentrations, indicating incomplete mixing. However, the sizes of the possible suspending Mb particles are much smaller than the typical wavelength of the THz radiation (~300 $\mu$m) so that the scattering loss is not a major effect here.

Samples with high water content strongly absorb THz radiation, necessitating very short but accurately known path lengths. We used commercially available cuvettes made of optical glass with sample compartment thicknesses of 100 and 200 $\mu$m. By comparing the absorption spectra from both path lengths, it was possible to extract the absorption coefficients of the Mb aqueous solution sample, as discussed below.

**II.2. Experimental Method.** The experimental setup of the THz spectrometer used in this work is the same as that described in our previous paper.[36] A simplified schematic is illustrated in Figure 1. A Ti:sapphire femtosecond (fs) laser with central wavelength at 800 nm and pulse width of 100 fs is used to pump the THz transmitter (Tx) and probe the THz receiver (Rx) to generate and detect the THz electric field, respectively. The THz pulse has a temporal profile extending many picoseconds (ps) after passing through the sample. The signal detected is a transient current proportional to the amplitude of the THz electric field. This current is converted into voltage in a lock-in current-to-voltage amplifier and processed as a time-domain waveform by a dedicated computer. The detected electric field is then fast Fourier transformed (FFT) to yield the frequency-domain spectrum.

Before FFT is applied, some manipulations of the time-domain waveform are necessary. First, a DC offset due to the data acquisition circuit on the waveform is subtracted. Then a cutoff time of about 10 ps after the main THz peak is applied and the waveform is truncated to remove satellite peaks resulting from reflection on the sample cell walls (1.2 mm of optical glass) that occur about 14 ps after the main peak and carry no significant information about the sample. Furthermore, to smooth the abruptness of the signal at the window edge due to truncation, some extrapolations based on the linear extension of the data points near the window edge are used. Finally, the time-domain waveform is zero-padded to 4096 points (including measured data of 3060 points) to increase the effective frequency resolution.

In THz-TDS experiments, thickness oscillations are always a concern because the wavelength of THz radiation is comparable to typical sample thicknesses. A reliable algorithm to extract the material parameters is crucial in the data analysis because multiple reflections on the interface between sample and sample cell interfere with the primary transmitted beam and complicate parameter extraction.[44] Caution must be used in the experiments as well as with data analysis procedures to ensure the results are free from such interference effects. For the Mb powder samples, the material parameter extraction procedure has been detailed in our previous paper.[36] For the Mb solution samples, as noted above, we used two rectangular cuvettes of different thicknesses as sample holders. Measurements were taken separately with both sample holders, and reproducible time-domain THz waveforms were obtained within experimental uncertainties. The data analysis scheme applied for Mb in solution is analogous to the method used by Kindt et al. for the measurements of liquid water and other polar liquids.[45] In contrast to their experiments in which the absorption measurements were taken for several path lengths at intervals of 50 or 100 $\mu$m and in the range of 50−1000 $\mu$m, only two cuvettes of different thicknesses (100 or 200 $\mu$m) were readily available for use as sample holders for Mb solutions in the current work, but these proved to be sufficient for reproducible measurements yielding established values for bulk water, for example. After FFT had been performed on the time-domain waveform to obtain the frequency-dependent amplitude $E(\omega)$ and phase $\phi(\omega)$ of the electric field, the following two formulas were used to find the absorption coefficient $\alpha(\omega)$ and refractive index $n(\omega)$ of each sample:[45,46]

$$\alpha(\omega) = \frac{\ln P_1(\omega) - \ln P_2(\omega)}{d} \quad (1)$$

$$n(\omega) = \frac{[\phi_2(\omega) - \phi_1(\omega)]c}{d\omega} + 1 \quad (2)$$

Here $P_1$ and $P_2$ and $\phi_1$ and $\phi_2$ are the transmission intensity ($P \propto E^2$) and phase shift at 100 and 200 $\mu$m path lengths, respectively; $c$ is the speed of light in a vacuum, and $d$ is 100 $\mu$m, the path length difference between the two cuvettes.

In applying eqs 1 and 2, it was assumed that the reflection and transmission coefficients due to the glass sample cell walls are identical and therefore can be divided out. The Fabry−Perot reflections on the sample cell walls occur 14 ps after the primary transmitted peak and can be removed by applying a time window 10 ps after the main peak. The first Fabry−Perot echo due to the sample itself is entangled with the main peak and cannot be separated by windowing. However, its amplitude is only about 0.1% of the main peak and assumed to be negligible. Therefore, the only differences between the two measurements

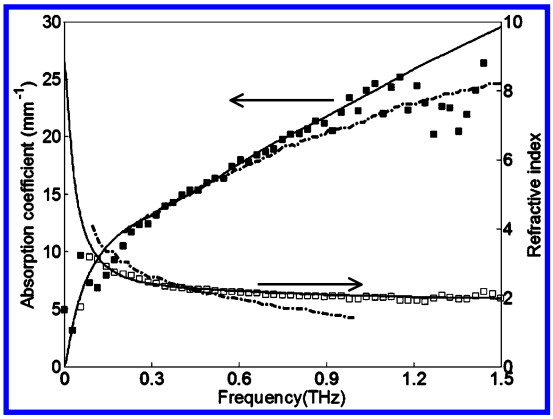


**Figure 2.** Absorption coefficient and refractive index of liquid water. The solid and open squares are the measured absorption coefficient and refractive index in this work, respectively. The solid and dashed lines are taken from refs 48 and 47 respectively.

are stronger absorption and larger phase shift for the longer path length, allowing the use of eqs 1 and 2 to extract the specimen parameters.

In this work, the deduced absorption coefficient and refractive index are averages over multiple measurements for each sample at each individual frequency. A standard deviation at each frequency is calculated from these multiple measurements. Although it was indicated in the work by Kindt et al.[45] that using only two path lengths may introduce significantly more errors in the optical constants than using variable path lengths, any such uncertainty in the current work proved to be significantly smaller than the standard deviations calculated from the multiple absorption scans (which were typically within ±5% of each data point).

## III. Results and Discussion

Before presenting experimental results for aqueous Mb solutions, we first validate the entire process by recording the THz absorption spectrum for liquid water and show good agreement with published data on absorption in this frequency range.[47,48] We then combine the previous results on Mb−water mixtures from 3.6 to 42 wt % water[36] with new measurements spanning from 70 to 98 wt % water. The absorption cannot be fit by a linear model combining the absorption properties of dry Mb and pure water. The enhanced Mb absorption is analyzed in terms of absorption per protein molecule (molar absorptivity), including explicitly the role of biological water.

**III.1. Far-Infrared Absorption Spectrum of Liquid Water.** Using the two sample holders with different path lengths, we obtained the absorption coefficient and refractive index data for liquid water as shown in Figure 2. These are compared to results from previous researchers.[47,48] The measurements by Thrane et al.[47] were based on THz reflection spectroscopy. Agreement is good in the frequency range from 0.3 to 1.2 THz. Due to increasingly strong absorption from the sample above 1.2 THz, the transmitted THz signal falls below the instrumental noise level, resulting in poor signal-to-noise ratio. The signal below 0.3 THz appears to suffer from a systematic truncation effect, which results from the application of a rectangular cutoff window on the time-domain waveform and makes the FFT results suspect. In this work, we will consider only the frequency range from 0.3 to 1.2 THz. For the refractive index, the agreement is excellent from 0.1 to 1.5 THz. Although refractive index data were also obtained for all of the Mb samples under study, they remain roughly unchanged within experimental uncertainties as a function of water content at each frequency and will not be analyzed here.

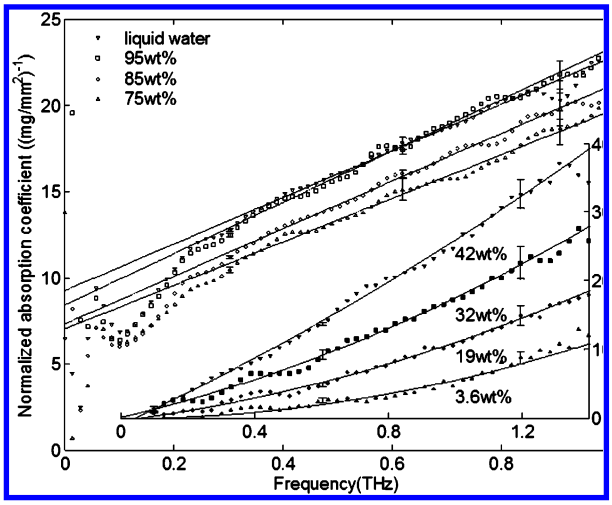


**Figure 3.** Absorption spectra of Mb solutions at different water concentrations: (▽) liquid water; (□) 95 wt %; (◇) 85 wt %; (△) 75 wt %; (▼) 42 wt %; (■) 32 wt %; (◆) 19 wt %; (▲) 3.6 wt %. The solid line is a polynomial fit for each sample based on the frequency range with good signal-to-noise ratio. For Mb solutions, this range is from 0.3 to 0.8 THz. For Mb powders, this range is from 0.1 to 1.2 THz. It can be seen that the Mb powder absorption spectrum can be fitted by a quadratic curve[36] and that the Mb solution absorption spectrum is better fitted by a linear curve. The fitting curves will be used as the basis for the discussions in section III.3. The inset shows the absorption spectra of Mb powders at different water concentrations.[36]

These measurements on water help to establish the general validity of the procedures subsequently employed on the Mb−water mixtures.

**III.2. Far-Infrared Absorption Spectrum of Mb Powders and Mb Aqueous Solutions.** The absorption spectra of Mb aqueous solutions at water concentrations of 75, 85, and 95 wt % are shown in Figure 3, along with the liquid water spectrum. Absorption spectra of Mb powders at hydration levels ranging from 3.6 to 42 wt %[36] are included in the inset. The absorption coefficient is normalized to the sample density to take into account the difference in the sample packing condition, particularly for Mb powders. The sample density can be determined to ±2% relative error by precisely measuring the mass of a certain volume of Mb powder or solution. The error bars shown on selected frequencies are the standard deviations of the absorption coefficient obtained from multiple measurements divided by the corresponding sample density.

The absorption for 95 wt % water is almost indistinguishable from that of pure water. Mb solutions at 85 and 75 wt % water demonstrate reduced absorption compared with pure water, a result of the substitution of polar water molecules by the relatively nonpolar Mb molecule.

Figure 3 includes a polynomial fit to each absorption curve, drawn through the weak oscillations that likely are residual effects of interference in the sample holder. The absorption spectrum of each Mb powder is fit by a quadratic curve over the frequency range from 0.1 to 1.2 THz.[36] For the Mb solutions and liquid water, better fits are obtained with a simple straight line over the data from 0.3 to 0.8 THz, where the signal-to-noise ratio is excellent.

As noted in our previous work, THz absorption in these Mb−water mixtures is a smooth function of frequency that is largely determined by the water content.[36] No identifiable features that might be associated with protein normal modes can be seen,

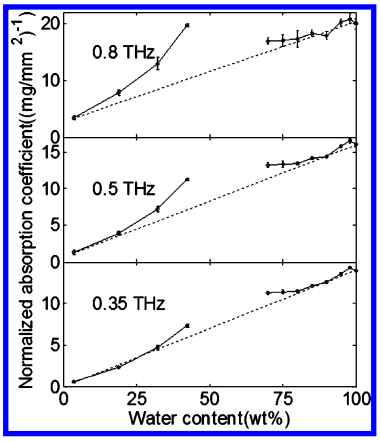


**Figure 4.** Normalized areal absorption coefficient of Mb−water mixtures as a function of water content at selected frequencies (0.35, 0.5, and 0.8 THz). The absorption coefficients used here for each sample are taken from the fitting curves presented in Figure 3, to average over any uncertainties in the measurements. The measured data points are denoted by open circles with an error bar on each data point. The solid lines connecting the high and low water content data points are used to guide the eyes. The gap left between 42 and 70 wt % samples indicates that we do not have data points for the intermediate water contents. The dotted straight liness are the results calculated on the basis of an ideal model in which the Mb molecules and water molecules are assumed to be two non-interacting species. It can be seen that increased absorption is observed for many of the samples measured at all of the selected frequencies, as compared with the ideal model.

perhaps due to inhomogeneous broadening from conformational disorder or other water-related factors.

In the following analysis, absorption coefficients are taken from the fits instead of the original spectra, in order to average over experimental uncertainties and remnant oscillation effects in the region from 0.3 to 0.8 THz.

**III.3. Mb Absorption in an Ideal Non-interacting Model.** Using the fits from Figure 3 to describe the Mb−water absorption measurements, we replot the results for fixed frequencies of 0.35, 0.5, and 0.8 THz in Figure 4. The error bar on each data point is the same error bar presented in Figure 3. The solid lines connecting the high and low water content data points are used to guide the eye. For comparison we include the straight dashed line corresponding to a non-interacting model, where absorption would depend only on the fractional molar concentrations (defined as the number of moles per unit volume) of Mb and water. That is, the absorption coefficient $\alpha$ of the mixture is given by the linear combination of the two constituents

$$\alpha = \sigma_{H_2O} M_{H_2O} + \sigma_{Mb} M_{Mb} \quad (3)$$

where $\sigma_{H_2O}$ and $\sigma_{Mb}$ are the molar absorptivity of pure water and dry Mb, respectively. $M_{H_2O}$ and $M_{Mb}$ are the fractional molar concentrations of water and Mb in the Mb−water mixture system, respectively, which are given by

$$M_{H_2O} = \frac{x\rho}{MW_{H_2O}} \quad (4)$$

and

$$M_{Mb} = \frac{(1-x)\rho}{MW_{Mb}} \quad (5)$$

where $\rho$ and $x$ are the sample density and water content, respectively. $MW_{H_2O} = 18$ g/mol and $MW_{Mb} = 16952$ g/mol are the molecular weights of water and Mb, respectively. Substituting eqs 4 and 5 into eq 3 and dividing both sides by the sample density $\rho$, we will obtain the normalized absorption coefficient $\alpha/\rho$ as a linear function of water content $x$, which is the straight line shown in Figure 4.

**TABLE 1. Absorption Coefficients[a] of Liquid Water and Dry Myoglobin at Selected Frequencies**

| | absorption coefficient | | | |
|---|---|---|---|---|
| | liquid water[48] | | dry Mb (this work) | |
| frequency (THz) | $\alpha$ ($mm^{-1}$) | $\sigma$ $(mmol/mm^2)^{-1}$ | $\alpha$ ($mm^{-1}$) | $\sigma$ $(mmol/mm^2)^{-1}$ |
| 0.35 | 14.0 | $2.52 \times 10^2$ | $0.01 \pm 0.01$ | $0.27 \times 10^4$ |
| 0.5 | 16.0 | $2.88 \times 10^2$ | $0.06 \pm 0.01$ | $1.66 \times 10^4$ |
| 0.8 | 20.4 | $3.67 \times 10^2$ | $0.16 \pm 0.01$ | $4.44 \times 10^4$ |

[a] The absorption coefficients for dry Mb are obtained from a THz-TDS measurement of Mb powder containing about 1 wt % water, achieved by lengthy drying in a desiccator. The error included in the table for the absorption coefficient of dry Mb is the standard deviation obtained from multiple measurements. The absorption coefficient is also expressed in molar absorptivity, which will be used to evaluate eq 3.

The molar absorptivity, by definition, is the absorption coefficient divided by the sample molar concentration and describes the specimen absorptivity on a molecular basis. For liquid water, the absorption coefficients are taken from the published values.[48] For frequencies at which data are not available, cubic spline interpolation is used to obtain the absorption coefficients. For Mb, we used values obtained from a THz-TDS measurement of Mb powder containing about 1 wt % water, achieved by lengthy drying in a desiccator. The absorption coefficients used for liquid water and dry Mb are listed in Table 1 for selected frequencies at 0.35, 0.5, and 0.8 THz. The error included in the table for the absorption coefficient of dry Mb is the standard deviation obtained from multiple measurements. Also listed in Table 1 are the molar absorptivities of liquid water and dry Mb for evaluating eq 3. The molar absorptivity of dry Mb is about 2 orders of magnitude larger than that of liquid water, due to the much larger molecular size of Mb.

In Figure 4, there are no data points for water content between 42 and 70 wt %. For powder samples being brought into equilibrium with various saturated salt solutions, we failed to obtain samples with water content greater than 42 wt %; at that concentration, the Mb powder had converted into a dense paste. Earlier measurements of dielectric response[49] deduced a maximum level of 0.6 g of water per gram of Mb, corresponding to 37.5 wt % water and in reasonable agreement with our 42 wt % result. For solution samples obtained by mixing Mb powder with bulk water, although it is indicated in the Material Safety Data Sheet (MSDS) of horse heart Mb that its solubility in liquid water is only 20 mg/mL,[50] researchers typically obtain concentrations of 170 mg/mL (about 85 wt % water content) at pH 6.9,[49] which is roughly the same as our dissolving limit. In our case, the concentrations from 98 to 80 wt % appeared to be uniform solutions. For the specimens at 75 and 70 wt % water, there was some visual evidence of undissolved Mb. However, the results of the subsequent analysis are not materially affected even if we leave out these two samples.

Deviations of the normalized absorption from the non-interacting model show enhanced THz absorption. This is contrary to expectations, because substantial evidence exists that biological water has a reduced effective dipole moment and would tend to suppress the THz absorption, relative to the non-interacting model. Calculations suggest that the effective dipole

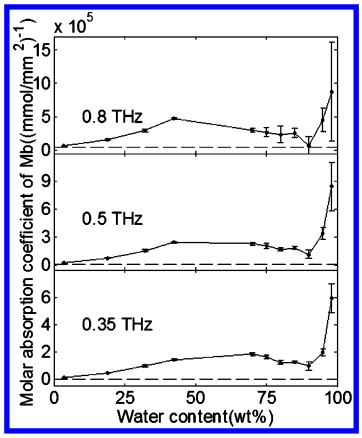


**Figure 5.** Molar absorptivity of Mb as a function of water content at frequencies of 0.35, 0.5, and 0.8 THz. The solid circles with error bars connected by solid line are the actual data points. The dashed line denotes the absorptivity of dry Mb as a base level. An enhanced molar absorption is seen throughout, with a dramatic increase at the dilute limit.

moment for a water molecule falls from 2.5 D in the bulk state to about 0.8 D for the region of biological water around a protein, presumably caused by water at surface sites being rotationally hindered.[2,51] The 0.8 D effective dipole moment of protein-bound water represents a reduced response of water molecules to applied electric field compared with free bulk water, which will show up as an absorption decrease in our case. Adding this known interaction to the non-interacting model should lead to suppression, not enhancement, of the absorption for the whole system.

**III.4. Mb Absorption in an Interacting Model.** For further analysis it is useful to consider how the absorption per protein molecule changes with water content. For the driest Mb powders, the only water molecules would be those few entrained in the protein interior and would contribute little to THz absorption. As water content increases, more water molecules would be at protein surfaces and would function as biological water. For Mb dissolved in bulk water, only the fraction corresponding to one to two molecular layers surrounding each protein molecule would be biological water, with the remainder expected to be simply bulk water. We construct a model describing these species of water and use it to extract the effective absorption per protein molecule from the data.

This interacting model makes the following specific assumptions: (i) The very dry specimen with 3.6 wt % water will be treated as Mb alone. That is, the first 3.6 wt % of the water is non-absorbing because all of the water molecules are basically confined within the protein structure. (ii) For the powder specimens with 19, 32, and 42 wt % water, we assume that all of this water is biological water for which absorption is a function of concentration. For the 19 wt % specimen we assume water absorbs at 10% of the bulk water value, for the 32 wt % water specimen we assume 20% of the bulk water value, and for the 42 wt % sample we assume 30%, corresponding to a 0.8 D dipole moment. (iii) All water beyond the first 42 wt % absorbs as bulk water, corresponding to a 2.5 D dipole moment.

Although this model may seem arbitrary, our qualitative conclusions do not strongly depend on the choice of parameters. Choosing very different numbers for the absorption of biological water leads to only modest changes in the curves, without affecting the conclusions. In the following analysis, we will illustrate the results based on only the above assumptions.

The total absorption coefficient is thus modeled as

$$\alpha = \sigma_{Mb}M_{Mb} + \sigma_{free-H_2O}M_{free-H_2O} + \sigma_{bio-H_2O}M_{bio-H_2O} \quad (6)$$

where $\sigma_{Mb}$, $\sigma_{free-H_2O}$, and $\sigma_{bio-H_2O}$ are the molar absorptivities of Mb, bulk free water, and biological bound water, respectively. $M_{Mb}$, $M_{free-H_2O}$, and $M_{bio-H_2O}$ are the fractional molar concentrations of Mb, bulk free water, and biological bound molecules water, respectively. Equation 6 applies to a given frequency. For selected frequencies at 0.35, 0.5, and 0.8 THz, $\sigma_{free-H_2O}$ will take the values in Table 1 and $\sigma_{bio-H_2O}$ will be calculated according to the assumptions made above as a function of water concentration. The molar absorptivity of Mb, $\sigma_{Mb}$, can then be calculated.

The resulting molar absorptivity of Mb molecule is plotted in Figure 5 as a function of water content and frequency. The baseline absorption of dry Mb (1.2 wt % water) is shown as the dashed line; note that adding water increases the molar absorption by more than an order of magnitude. Also shown in Figure 5 on each data point is an error bar; following is a discussion of the sources of uncertainty.

Rearrangement of eq 6 gives

$$\sigma_{Mb} = \frac{\alpha - \sigma_{free-H_2O}M_{free-H_2O} - \sigma_{bio-H_2O}M_{bio-H_2O}}{M_{Mb}} \quad (7)$$

where $\sigma_{free-H_2O}$ and $\sigma_{bio\_H_2O}$ assume the modeled values and hence do not cause random errors. The main sources of random error result from the measurements of $\alpha$, $M_{Mb}$, $M_{free-H_2O}$, and $M_{bio-H_2O}$. The standard deviation of $\sigma_{Mb}$, $\Delta\sigma_{Mb}$, can be written as

$$\Delta\sigma_{Mb} = \sqrt{\left(\frac{\Delta\alpha}{M_{Mb}}\right)^2 + \left(\frac{\Delta M_{Mb}}{M_{Mb}}\right)^2 {\sigma_{Mb}}^2 + \left(\frac{\Delta M_{free-H_2O}}{M_{Mb}}\right)^2 {\sigma_{free-H_2O}}^2 + \left(\frac{\Delta M_{bio-H_2O}}{M_{Mb}}\right)^2 {\sigma_{bio-H_2O}}^2} \quad (8)$$

where $\Delta\alpha$, $\Delta M_{Mb}$, $\Delta M_{free-H_2O}$, and $\Delta M_{bio-H_2O}$ are the standard deviations of $\alpha$, $M_{Mb}$, $M_{free-H_2O}$, and $M_{bio-H_2O}$, respectively.

In the present work, the measurements showed that

$$\frac{\Delta\alpha}{M_{Mb}} \sim 15\%\ \sigma_{Mb} \quad (9)$$

which is dominated by the standard deviation for $\alpha$ calculated at each frequency from the multiple repeated THz-TDS scans except for the lowest concentrations, at which the small size of $M_{Mb}$ becomes the dominant factor. The last three terms all have the same order of magnitude.

$$\frac{\Delta M_{Mb}}{M_{Mb}}\sigma_{Mb} \sim \frac{\Delta M_{free-H_2O}}{M_{Mb}}\sigma_{free-H_2O} \sim \frac{\Delta M_{bio-H_2O}}{M_{Mb}}\sigma_{bio-H_2O} < 3\%\ \sigma_{Mb} \quad (10)$$

The contribution from these three terms is small because the uncertainty in measuring the masses involved, even at low Mb concentrations, is much smaller than the uncertainty in the THz-TDS scans. Thus, the uncertainty in $\sigma_{Mb}$ is dominated by the experimental error in the total absorption coefficient $\alpha$ (94% contribution), so that $\Delta\sigma_{Mb}$ can be approximated as

$$\Delta\sigma_{Mb} \approx \frac{\Delta\alpha}{M_{Mb}} \quad (11)$$

which is the error bar shown on each data point in Figure 5.

The error bars generally increase with frequency and water content because the standard deviation in the absorption coefficient increases with frequency, and the molar concentration of Mb decreases with water content.

**III.5. Discussion.** The absorption per Mb molecule shows two clear trends: a general enhanced absorption relative to dry Mb and a sharp increase at high water content.

Absorption of THz radiation requires a change in the electric dipole moment of the absorber.[52] It has previously been speculated that the presence of water might enhance the mobility of various amino acid side chains along the protein, enhancing their response to the applied field. Water is therefore believed to increase the local flexibility of the protein molecule and is described as a "plasticizer" by Pethig et al.[14,15] in their studies of lysozyme and cytochrome *c*. This enhanced side-chain flexibility could be related to the generally increased molar absorption seen in Figure 5.

The dramatic increases seen above 90 wt % water are especially surprising. Although it is consistent with results reported for BSA above 95 wt % water,[41] the experimental uncertainties in that measurement could not exclude the possibility of no change in molar absorptivity.

For a possible explanation, we consider interactions between Mb molecules in a dilute aqueous solution. The average separation between Mb molecules at 90 wt % concentration is about 6.5 nm. Given that the protein radius is around 1.5 nm if its shape is approximated as a sphere and the shell of biological water is usually considered to be less than 0.5 nm thick,[49] this average separation corresponds to a significant amount of bulk water already between adjacent proteins. It is likely, however, that nearby proteins interact with each other, perhaps forming pairs or even instantaneous networks of weak bonds that are sufficient to suppress the full polarizability of a protein molecule in the dilute limit. The 90 wt % concentration may then mark the onset of there being a finite fraction of Mb molecules free of protein−protein interactions. This would be manifested, for example, as a decrease in the solute molecule orientational relaxation time, which facilitates the alignment of Mb molecules with the incoming electromagnetic field. This would enhance the interaction between Mb molecules and the incident radiation field and result in an increased Mb molar absorptivity with increasing water content.

## IV. Conclusions

Absorption of electromagnetic radiation from 0.1 to 1.2 THz has been measured for Mb−water mixtures, using THz time-domain spectroscopy. A non-interacting model in which absorption depends linearly on the number of Mb and water molecules does not fit the data. The expected reduction in absorption due to biological water that strongly interacts with the protein is not observed; on the contrary, enhanced absorption is seen over a broad range of compositions and frequencies. A simple model for incorporating the reduced absorption of biological water and using measured values for the remaining bulk water allows the extraction of the molar absorptivity of Mb, that is, the absorption per Mb molecule as a function of water content. This shows generally enhanced absorption plus a sharp increase above 90 wt % water. This response may be associated with enhanced flexibility of the protein for intermediate water concentrations, plus greater rotational freedom at high water content.

These results provide quantitative data for the response of a specific protein to electromagnetic radiation in the THz range. Understanding the microscopic mechanisms for enhanced absorption may be important for accurate modeling of possible deleterious effects of electromagnetic radiation on biological materials.

**Acknowledgment.** We thank Professor Andrew M. Weiner for many contributions to the experimental aspects of this research. This work was supported in part by the Integrated Detection of Hazardous Materials Program (Purdue University) and the National Science Foundation (PHY-9988763).

## References and Notes

(1) Rupley, J. A.; Careri, G. *Adv. Protein Chem.* **1991**, *41*, 37.
(2) Pethig, R. *Annu. Rev. Phys. Chem.* **1992**, *43*, 177.
(3) Pethig, R. Dielectric studies of protein hydration. In *Protein−Solvent Interactions*; Gregory, R. B., Ed.; Dekker: New York, 1994; p 265.
(4) Sage, J. T.; Schomacker, K. T.; Champion, P. M. *J. Phys. Chem.* **1995**, *99*, 3394.
(5) Diehl, M.; Doster, W.; Petry, W.; Schober, H. *Biophys. J.* **1997**, *73*, 2726.
(6) Librizzi, F.; Viappiani, C.; Abbruzzetti, S.; Cordone, L. *J. Chem. Phys.* **2002**, *116*, 1193.
(7) Tarek, M.; Tobias, D. J. *Phys. Rev. Lett.* **2002**, *89*, 275501.
(8) Bizzarri, A. R.; Cannistraro, S. *J. Phys. Chem. B* **2002**, *106*, 6617.
(9) Yu, X.; Park, J.; Leitner, D. M. *J. Phys. Chem. B* **2003**, *107*, 12820.
(10) Svergun, D. I.; Richard, S.; Koch, M. H. J.; Sayers, Z.; Kuprin, S.; Zaccai, G. *Proc. Natl. Acad. Sci. U.S.A.* **1998**, *95*, 2267.
(11) Smith, J. C.; Merzel, F.; Bondar, A. N.; Tournier, A.; Fischer, S. *Philos. Trans. R. Soc. London Ser. B−Biol. Sci.* **2004**, *359*, 1181.
(12) Nandi, N.; Bagchi, B. *J. Phys. Chem. B* **1997**, *101*, 10954.
(13) Pal, S. K.; Peon, J.; Zewail, A. H. *Proc. Natl. Acad. Sci. U.S.A.* **2002**, *99*, 1763.
(14) Bone, S.; Pethig, R. *J. Mol. Biol.* **1982**, *157*, 571.
(15) Bone, S.; Pethig, R. *J. Mol. Biol.* **1985**, *181*, 323.
(16) Randall, J.; Middendorf, H. D.; Crespi, H. L.; Taylor, A. D. *Nature (London)* **1978**, *276*, 636.
(17) Tsai, A. M.; Neumann, D. A.; Bell, L. N. *Biophys. J.* **2000**, *79*, 2728.
(18) Neilson, G. W.; Mason, P. E.; Ramos, S.; Sullivan, D. *Philos. Trans. R. Soc. London Ser. A−Math. Phys. Eng. Sci.* **2001**, *359*, 1575.
(19) Dorbez-Sridi, R.; Cortes, R.; Mayer, E.; Pin, S. *J. Chem. Phys.* **2002**, *116*, 7269.
(20) Bon, C.; Dianoux, A. J.; Ferrand, M.; Lehmann, M. S. *Biophys. J.* **2002**, *83*, 1578.
(21) Otting, G.; Wuthrich, K. *J. Am. Chem. Soc.* **1989**, *111*, 1871.
(22) Otting, G.; Liepinsh, E.; Wuthrich, K. *Science* **1991**, *254*, 974.
(23) Otting, G.; Liepinsh, E. *Acc. Chem. Res.* **1995**, *28*, 171.
(24) Modig, K.; Liepinsh, E.; Otting, G.; Halle, B. *J. Am. Chem. Soc.* **2004**, *126*, 102.
(25) Haggis, G. H.; Buchanan, T. J.; Hasted, J. B. *Nature (London)* **1951**, *167*, 607.
(26) Singh, G. P.; Parak, F.; Hunklinger, S.; Dransfeld, K. *Phys. Rev. Lett.* **1981**, *47*, 685.
(27) Wei, Y. Z.; Kumbharkhane, A. C.; Sadeghi, M.; Sage, J. T.; Tian, W. D.; Champion, P. M.; Sridhar, S.; Mcdonald, M. J. *J. Phys. Chem.* **1994**, *98*, 6644.
(28) Suzuki, M.; Shigematsu, J.; Kodama, T. *J. Phys. Chem.* **1996**, *100*, 7279.
(29) Gerothanassis, I. P.; Birlirakis, N.; Karayannis, T.; Sakarellosdaitsiotis, M.; Sakarellos, C.; Vitoux, B.; Marraud, M. *Eur. J. Biochem.* **1992**, *31*, 693.
(30) Kandori, H.; Iwata, T.; Hendriks, J.; Maeda, A.; Hellingwerf, K. J. *Biochemistry* **2000**, *39*, 7902.
(31) McMullen, T. P. W.; Lewis, R. N. A. H.; McElhaney, R. N. *Biophys. J.* **2000**, *79*, 2056.
(32) Han, P. Y.; Tani, M.; Usami, M.; Kono, S.; Kersting, R.; Zhang, X. C. *J. Appl. Phys.* **2001**, *89*, 2357.
(33) Hu, B. B.; Nuss, M. C. *Optics Lett.* **1995**, *20*, 1716.
(34) Korter, T. M.; Balu, R.; Campbell, M. B.; Beard, M. C.; Gregurick, S. K.; Heilweil, E. J. *Chem. Phys. Lett.* **2006**, *418*, 65.
(35) Siegrist, K.; Bucher, C. R.; Mandelbaum, I.; Walker, A. R. H.; Balu, R.; Gregurick, S. K.; Plusquellic, D. F. *J. Am. Chem. Soc.* **2006**, *128*, 5764.
(36) Zhang, C. F.; Tarhan, E.; Ramdas, A. K.; Weiner, A. M.; Durbin, S. M. *J. Phys. Chem. B* **2004**, *108*, 10077.
(37) Markelz, A. G.; Roitberg, A.; Heilweil, E. J. *Chem. Phys. Lett.* **2000**, *320*, 42.
(38) Markelz, A.; Whitmire, S.; Hillebrecht, J.; Birge, R. *Phys. Med. Biol.* **2002**, *47*, 3797.
(39) Knab, J.; Chen, J. Y.; Markelz, A. *Biophys. J.* **2006**, *90*, 2576.

(40) Chen, J. Y.; Knab, J. R.; Cerne, J.; Markelz, A. G. *Phys. Rev. E* **2005**, *72*, 040901.
(41) Xu, J.; Plaxco, K. W.; Allen, S. J. *Protein Sci.* **2006**, *15*, 1175.
(42) Whitmire, S. E.; Wolpert, D.; Markelz, A. G.; Hillebrecht, J. R.; Galan, J.; Birge, R. R. *Biophys. J.* **2003**, *85*, 1269.
(43) Globus, T. R.; Woolard, D. L.; Khromova, T.; Crowe, T. W.; Bykhovskaia, M.; Gelmont, B. L.; Hesler, J.; Samuels, A. C. *J. Biol. Phys.* **2003**, *29*, 89.
(44) Duvillaret, L.; Garet, F.; Coutaz, J. L. *IEEE J. Sel. Top. Quantum Electron.* **1996**, *2*, 739.
(45) Kindt, J. T.; Schmuttenmaer, C. A. *J. Phys. Chem.* **1996**, *100*, 10373.
(46) Venables, D. S.; Schmuttenmaer, C. A. *J. Chem. Phys.* **1998**, *108*, 4935.
(47) Thrane, L.; Jacobsen, R. H.; Jepsen, P. U.; Keiding, S. R. *Chem. Phys. Lett.* **1995**, *240*, 330.
(48) Querry, M. R.; Wieliczka, D. M.; Segelstein, D. J. Water ($H_2O$). In *Handbook of Optical Constants of Solids*; Palik, E. D., Ed.; Academic Press: San Diego, CA, 1991; Vol. II., p 1059.
(49) Grant, E. H.; Mcclean, V. E. R.; Nightingale, N. R. V.; Sheppard, R. J.; Chapman, M. J. *Bioelectromagnetics* **1986**, *7*, 151.
(50) Sigma-Aldrich. Material Safety Data Sheet of Myoglobin from Equine Heart; http://www.sigmaaldrich.com/catalog/search/productdetail/sigma/M1882.
(51) Gascoyne, P. R. C.; Pethig, R. *J. Chem. Soc., Faraday Trans. 1* **1981**, *77*, 1733.
(52) Guillot, B. *J. Chem. Phys.* **1991**, *95*, 1543.